



# Ammonia and nitrite oxidation in the upper euphotic zone of the oligotrophic Red Sea

Eyal Rahav<sup>1,2,3</sup>, Scott D. Wankel<sup>4</sup>, and Adina Paytan<sup>2</sup>

<sup>1</sup>Israel Oceanographic and Limnological Research, Haifa, Israel

<sup>2</sup>Institute of Marine Science, University of California, Santa Cruz, CA, USA

<sup>3</sup>Department of Earth and Environmental Science, Ben-Gurion University of the Negev, Beer Sheva, Israel

<sup>4</sup>Marine Chemistry and Geochemistry Department, Woods Hole Oceanographic Institution, Woods Hole, Massachusetts, USA

**Correspondence:** Eyal Rahav (eyrahav@ucsc.edu, eyal.rahav@ocean.org.il)

Received: 12 February 2026 – Discussion started: 6 March 2026

Revised: 4 June 2026 – Accepted: 5 June 2026 – Published: 24 June 2026

**Abstract.** Nitrification is widely understood to be inhibited by light in the surface ocean, however, increasing evidence indicates its occurrence at low levels at many sites. The extent to which nitrification remains active in the euphotic zone could have important implications to new production calculations, yet it remains understudied. Here, we quantified ammonia and nitrite oxidation rates in the euphotic zone of the Gulf of Aqaba (Northern Red Sea) from late spring to late summer and examined environmental controls and implications for dark carbon fixation (chemoautotrophy) and new production. Both ammonia and nitrite oxidation were detectable throughout the euphotic zone ( $\sim 0.1\text{--}0.8\text{ nmolNL}^{-1}\text{d}^{-1}$ ). Overall, rates were low in the highest-irradiance surface waters and increased with depth. Integrated rates over the entire euphotic zone ( $24\text{--}56\text{ }\mu\text{molNm}^{-2}\text{d}^{-1}$ ) were among the lowest reported for oligotrophic regions globally. This reflects extremely low substrate concentrations and intense, though not complete, photo-inhibition. Ammonia and nitrite oxidation together supported  $< 2\%$  of dark carbon fixation rates, suggesting other processes, not accounted for, drive this chemoautotrophic activity. Depth-resolved correlations with environmental parameters highlight light, temperature, and substrate availability as key regulators of both processes. Our results show that nitrification in the Gulf of Aqaba operates at the lower bounds of global euphotic zone rates and is loosely coupled to carbon cycling. These findings underscore the need to better resolve nitrification dynamics in ultra-oligotrophic, rapidly warming, seas to refine estimates of

new production and chemoautotrophic carbon assimilation under future ocean conditions.

## 1 Introduction

Nitrification, the sequential oxidation of ammonium ( $\text{NH}_4^+$ ) to nitrite ( $\text{NO}_2^-$ ) followed by the oxidation of nitrite to nitrate ( $\text{NO}_3^-$ ), is a microbially mediated process central to the regulation of nitrogen availability across nearly all aquatic environments, linking the most reduced and oxidized states of nitrogen (Ward, 2008). Although nitrification does not change the absolute inventory of bioavailable nitrogen (N) in the oceans, it alters the balance among nitrogen species that serve as substrates for different organisms, thereby affecting phytoplankton species abundance and growth (Fawcett et al., 2011). Ammonia oxidation is carried out by ammonia-oxidizing archaea and bacteria (Francis et al., 2005; Wuchter et al., 2006), while nitrite oxidation is performed by nitrite-oxidizing bacteria (Mincer et al., 2007; Pachiadaki et al., 2017). Ammonia-oxidizing bacteria that perform the entire process have also been identified in freshwater, terrestrial, and coastal habitats, but have not yet been found in the open ocean (Daims et al., 2015; Fei et al., 2018; van Kessel et al., 2015).

Nitrification has been investigated across a wide range of marine settings, including the Atlantic (Clark et al., 2008, 2022), the Pacific (Wan et al., 2021; Wankel et al., 2007), and the Polar (Mdutyana et al., 2020; Shiozaki et al., 2019) ocean basins, as well as numerous coastal and estuarine

systems (Henriksen and Kemp, 1988; Herbert, 1999; Zhu et al., 2018). As a chemoautotrophic process, nitrification contributes to organic carbon production in the ocean interior (Middelburg, 2011; Pachiadaki et al., 2017), and may fuel bacterial carbon demand and support heterotrophic food-webs in the mesopelagic and bathypelagic water depths (Bayer et al., 2025). The activity of nitrifiers is known to be promoted or inhibited by many environmental factors (Ward, 2008), yet specific controls on its occurrence in the water column and broader ecological implications across different ocean settings remain poorly constrained (Tang et al., 2023). Additionally, because uptake of  $\text{NH}_4^+$  and  $\text{NO}_3^-$  has long served to differentiate between “regenerated” and “new” production, respectively (Eppley and Peterson, 1979), in situ production of  $\text{NO}_3^-$  by nitrification in the photic zone skews global estimates of new production and carbon export in the oceans (Yool et al., 2007; Wankel et al., 2007).

Here, we report ammonia and nitrite oxidation rates in the upper euphotic zone (surface and down to  $\sim 100$  m, representing 100 % to  $\sim 0.5$  %– $1.8$  % of surface irradiance, respectively) of the Gulf of Aqaba (GoA, Northern Red Sea) during late spring and throughout the summer season. Rates were compared with common environmental physiochemical and biological parameters to assess drivers of nitrification in this marine setting. Using these data, we provide estimates of the contribution of ammonia and nitrite oxidation to dark carbon fixation (DCF) and new production in the oligotrophic, warm and well-lit GoA.

## 2 Material and methods

Seawater was collected every 20 m throughout the euphotic zone (0–100 m depth) at an offshore, routinely monitored, station in the GoA (“Station A”, latitude 29.47 N, longitude 34.92 E). Ammonia and nitrite oxidation rates were assessed using stable  $^{15}\text{N}$  isotope enrichment incubations. Five monthly sampling events were performed spanning late spring/early summer (May) to late summer (September) in 2023, covering the period in which the GoA is characterized by oligotrophic N-poor conditions (Fuller et al., 2005; Mackey et al., 2007). Ancillary water column measurements included temperature, salinity, photosynthetic active radiation (PAR) (Seabird 19 Plus), inorganic nitrogen species concentrations ( $\text{NO}_2^-$ ,  $\text{NO}_3^-$ ,  $\text{NH}_4^+$ ), chlorophyll-*a*, and rates of photosynthesis and DCF.

### 2.1 Inorganic nitrogen species

Duplicate water samples for nitrite ( $\text{NO}_2^-$ ) and nitrate ( $\text{NO}_3^-$ ) were collected in 15 mL acid-clean polyethylene tubes directly from Niskin bottles. Prior to filling, the tube was thoroughly rinsed three times with sample water. After collection, samples were stored at 4 °C in the dark and analyzed the following day. Nitrite and nitrate concentrations

were determined colorimetrically following standard procedures (Grasshoff et al., 1999). Nitrite was measured directly using the Griess reaction, in which nitrite forms an azo dye after reaction with sulfanilamide and *N*-(1-naphthyl)ethylenediamine and is quantified spectrophotometrically ( $\lambda = 520$  nm). Nitrate was reduced to nitrite using a copper-coated cadmium reduction column and subsequently  $\text{NO}_2^- + \text{NO}_3^-$  was analyzed by the same azo-dye method. Nitrate concentrations were then calculated by difference. Analyses were performed using a Flow Injection Autoanalyzer system (FIA, Lachat Instruments Model QuikChem 8000). The analysis was automated, and peak areas were calibrated using standards prepared in nutrient-deplete 0.2- $\mu\text{m}$  filtered surface seawater from the GoA over a range of 0–100  $\text{nmol L}^{-1}$ . The detection limits were 10 and 20  $\text{nmol L}^{-1}$  for nitrite and nitrate, respectively, with typical analytical precision of  $\sim 20$   $\text{nmol L}^{-1}$ , consistent with previous measurements in the GoA (e.g., Mackey et al., 2011).

Samples for ammonia ( $\text{NH}_4^+$ ) concentration were collected directly from Niskin bottles into acid-washed plastic vials after rinsing 3 times with sample water. The collected samples were stored in 4 °C in the dark and analyzed within an hour after collection. Ammonia concentrations were determined using the orthophthaldialdehyde (OPA) method (Holmes et al., 1999), where samples were first incubated with a working reagent of OPA for 3 h and then measured fluorometrically (Turner Designs, Ex: 360 nm, Em: 420 nm). The detection limit was  $\sim 4$   $\text{nmol L}^{-1}$  (Meeder et al., 2012). Procedural blanks were routinely measured and subtracted from sample signals to account for background contamination. Note that calibration and quality control procedures were carried out during nutrient measurements. The analytical precision and detection limits were within the expected range for oligotrophic seawater measurements.

### 2.2 Ammonia and nitrite oxidation rates

Ammonia and nitrite oxidation rates were determined using stable isotope tracer incubations (Beman et al., 2011; Bristow et al., 2015; Ward, 1987). Seawater was collected into triplicate 1 L acid-cleaned transparent Nalgene bottles without headspace. The bottles were incubated on land for 24 h in aquarium tanks continuously supplied with running surface seawater, using neutral density screening nets simulating the light conditions of the collection depth (no change in spectra). For ammonia oxidation, samples were amended with  $^{15}\text{N}$ -labeled ammonium chloride ( $^{15}\text{NH}_4\text{Cl}$ ,  $> 98$  atom %; Cambridge Isotope Laboratories) at a concentration of  $\sim 20$   $\text{nmol L}^{-1}$  which is sufficient to yield a quantifiable signal while potentially introducing some degree of tracer perturbation (discussed below). For nitrite oxidation, samples were amended with  $\sim 5$   $\text{nmol L}^{-1}$  of  $^{15}\text{N}$ -labeled sodium nitrite ( $^{15}\text{NO}_2^-$ ,  $> 98$  atom %), thus minimally perturbing the in situ nitrite pool. At the end of the incubation, subsamples were filtered onto a Supor 0.22  $\mu\text{m}$  (47 mm) fil-

ter using gentle filtration, and the filtrate ( $< 0.22\ \mu\text{m}$ ) was kept frozen in the dark at  $-20\ ^\circ\text{C}$  until analysis. For ammonia oxidation, the presence of  $^{15}\text{NO}_2^-$  in the total dissolved nitrite pool was quantified by isotope ratio mass spectrometry (IRMS).

For nitrite oxidation, we quantified the  $^{15}\text{NO}_3^-$  in the dissolved nitrate pool after conversion to nitrous oxide with subsequent IRMS analysis. The azide method (McIlvin and Altabet, 2005) and the denitrifier method (Casciotti et al., 2002; Sigman et al., 2001), with technical updates for low-concentration analysis (McIlvin and Casciotti, 2011), are well established for isotopic analysis of nitrite and nitrate in oligotrophic seawater. Prior to denitrifier analysis, nitrite was removed from nitrate samples using the sulfamic acid procedure (Granger and Sigman, 2009) to ensure that the  $^{15}\text{N}$  signal reflected only the nitrate pool. Aliquots of 2–10 mL were introduced per denitrifier vial depending on ambient  $\text{NO}_3^-$  concentration, consistent with the volume constraints of Sigman et al. (2001) and McIlvin and Casciotti (2011). For surface samples with the lowest  $\text{NO}_3^-$  concentrations sequential injections of multiple aliquots from the same filtrate were used to accumulate sufficient N mass per vial, while for deeper samples with higher  $\text{NO}_3^-$  single injections of 2–5 mL were sufficient. Given that ambient  $\text{NO}_3^-$  and  $\text{NO}_2^-$  concentrations in GoA surface waters approached, or were below, the validated concentration ranges of these methods, the analyses were performed with careful attention to blank correction. Accordingly, rates derived from near-surface, low-concentration samples were interpreted conservatively. For sequential-injection analyses of low-concentration surface samples, multiple small-volume aliquots from the same 1 L filtrate were introduced into the same denitrifier vial to accumulate sufficient N mass, and the cumulative bacterial blank was estimated based on injection number and subtracted accordingly; samples where the  $^{15}\text{N}$  signal could not be distinguished from the cumulative blank were excluded and treated as below the detection limit. In the most oligotrophic surface samples these established approaches were applied near their practical detection limits, and  $^{15}\text{N}$  enrichments should therefore be regarded as conservative minimum estimates rather than evidence that the bacterial and azide methods are routinely robust at concentrations of only a few tens of  $\text{nmol L}^{-1}$ .

Killed controls poisoned with  $\text{HgCl}_2$  from each collection depth were incubated in parallel to the experimental bottles to account for any abiotic transformations and subtracted from the “live” bottles. Rates in the “mercury-killed” controls were typically negligible relative to the “live” bottles (usually  $< 0.05\ \text{nmol NL}^{-1}\ \text{d}^{-1}$ ). The resulting detection limit, which was defined as the mean killed-control rate plus three standard deviations, corresponded to  $0.1\ \text{nmol NL}^{-1}\ \text{d}^{-1}$ . Rates below this threshold were considered indistinguishable from background signal and were interpreted as “below detection”. This operational detection limit is based on the variability of killed controls and back-

ground signals and does not represent a full validation of isotope analysis at ambient nitrite or nitrate concentrations of only a few tens of  $\text{nmol L}^{-1}$ .

Rates of ammonia and nitrite oxidation were calculated following previous studies (Beman et al., 2011; Bristow et al., 2015; Ward, 1987) as shown in Eqs. (1)–(3):

$$\text{Ammonia oxidation} = \frac{\Delta(\text{atm } \%^{15}\text{NNO}_2) \times [\text{NO}_2]_{\text{final}}}{t \times F(\text{NH}_4)} \quad (1)$$

$$\text{Nitrite oxidation} = \frac{\Delta(\text{atm } \%^{15}\text{NNO}_3) \times [\text{NO}_3]_{\text{final}}}{t \times F(\text{NO}_2)} \quad (2)$$

$$F \text{ substrate} = \frac{[\text{15 N substrate}]_{\text{added}}}{[\text{Substrate ambient}] + [\text{Substrate added}]} \quad (3)$$

Where,  $\Delta(\text{atm } \%^{15}\text{N NO}_2^-)$  or  $\Delta(\text{atm } \%^{15}\text{N NO}_3^-) = \text{atom } \% \text{ excess } ^{15}\text{N}$  in the nitrite or nitrate pool relative to natural abundance;  $[\text{NO}_2^-]_{\text{final}}$  or  $[\text{NO}_3^-]_{\text{final}} = \text{final concentration of the nitrite or nitrate pool (nmol L}^{-1}\text{)}$ ;  $t = \text{time (d)}$ ;  $F_{\text{NH}_4}$  or  $F_{\text{NO}_2} = \text{fractional } ^{15}\text{N}$  enrichment of the ammonia or nitrite substrate pool.

Note that for the ammonia oxidation rates we added tracer additions which correspond to 30%–50% of the ambient  $\text{NH}_4^+$  concentrations. While we aimed to minimize substrate perturbation, such additions are inherently challenging in ultra-oligotrophic systems, where even low absolute tracer concentrations can represent a substantial fraction of the ambient pool (Zheng et al., 2020). Consequently, the reported rates should be considered as potential rates under moderately enriched conditions rather than strictly in situ rates (Dodds and Jones, 1987). Additionally, incubations were conducted over 24 h, which may allow for processes such as ammonia regeneration, microbial turnover, and grazing to influence substrate availability and isotopic dilution. Although  $\text{HgCl}_2$ -poisoned controls and parallel measurements were used to account for abiotic and background signals, these incubations cannot fully resolve short-term dynamics or transient coupling between regeneration and oxidation processes. These methodological constraints are inherent to low-rate measurements in oligotrophic systems (Ward, 1985) and should be considered when interpreting the results. Another potential caveat arising from the 24 h incubation is the potential production of unlabelled nitrite via phytoplankton nitrate reduction (e.g., Travis et al., 2024) thereby diluting the  $^{15}\text{NO}_2^-$  pool leading to an underestimation of both ammonia and nitrite oxidation rates. In the present study, however, primary production and ambient nitrite concentrations were low, suggesting that this effect was likely limited in magnitude.

### 2.3 Photosynthesis and Dark Carbon Fixation (DCF)

Photosynthesis and chemoautotrophic DCF rates were measured using  $\text{NaH}^{14}\text{CO}_3$  incorporation method (Stemann-Nielsen, 1952) with minor modifications (Reich et al., 2024,

2026). Triplicate seawater samples were collected from Niskin bottles in 50 mL acid-washed falcon tubes and spiked with a diluted “working solution” of  $\text{NaH}^{14}\text{CO}_3$  (Perkin Elmer, specific activity  $56 \text{ mCi mmol}^{-1}$ ) at a final radioisotope dilution of  $1 : 10^4 v : v$ . Tubes were incubated in the same tanks and under the same conditions used for the ammonia and nitrite oxidation measurements with one exception – the DCF bottles were first covered with aluminum foil to prevent light penetration. The tubes were incubated for 24 h before being filtered onto GF/F filters ( $0.7 \mu\text{m}$  nominal pore size, 25 mm diameter) using low vacuum pressure ( $< 50 \text{ mmHg}$ ). The filters were placed in glass scintillation vials and  $50 \mu\text{L}$  of 37 % hydrochloric acid was added to remove the non-fixed  $^{14}\text{C}$ -bicarbonate overnight. Scintillation cocktail (5 mL, ULTIMA-GOLD) was then added to each vial and samples were counted using a TRI-CARB 4810 TR (Packard) liquid scintillation counter. Additional  $T_0$  blanks were prepared by spiking bottles with  $\text{NaH}^{14}\text{CO}_3$  and filtering immediately (without incubation). Blanks consistently yielded negligible activity. Added activity was measured by withdrawing  $50 \mu\text{L}$  from random spiked bottles (immediately after dosing and before incubation) and adding it onto a new GF/F filter with  $50 \mu\text{L}$  of ethanolamine ( $\text{pH} \approx 12$ ) followed by scintillation cocktail and counting immediately.

Photosynthesis was calculated as the difference between the disintegration per minute (DPM) measured in the samples incubated under ambient irradiance and the dark bottles. DCF and photosynthesis rates were calculated based on the Bermuda Atlantic Time-series Study (BATS) protocol using the following Eq. (4):

$$\text{Production} = \frac{(\text{DPM-blank})}{V} \times \text{DIC} \times \frac{\text{AA vol}}{\text{TDPM}} \times f \times \frac{1}{t} \quad (4)$$

Where, DPM equals the disintegrations per minute,  $V$  = the filtered volume (50 mL), DIC is the dissolved inorganic carbon in seawater ( $\sim 25 \text{ mg CL}^{-1}$ ), similar to other oceanic sites, (Belkin et al., 2022), AA vol = Added activity volume ( $50 \mu\text{L}$ ), TDPM = Total  $^{14}\text{C}$  disintegration per minute,  $t$  = incubation time (24 h), and  $f$  = factor correcting isotope fractionation during uptake of  $^{14}\text{C}$  (1.05).

## 2.4 Chlorophyll-*a* analysis

Seawater samples (250 mL) were filtered onto Whatman GF/F filters at low pressure ( $< 150 \text{ mbar}$ ), placed in glass vials and frozen in the dark at  $-20^\circ\text{C}$ . Chlorophyll-*a* was extracted with 5 mL of cold acetone (90 %) overnight and determined by the non-acidification method (Welschmeyer, 1994) using a Turner Designs (Trilogy) fluorometer.

## 2.5 Statistical analysis

Pairwise relationships between environmental variables and process rates were evaluated using Pearson correlation coefficients calculated across all individual observations, including all sampled depths (0–100 m) and stations. No prior

averaging by depth or profile was applied. Because many variables co-vary with depth and season, these correlations should be interpreted as measures of co-variation rather than independent or causal relationships. Full Pearson correlation statistics ( $r$ ,  $r^2$ ,  $p$ -values) are provided in Tables S1 and S2 in the Supplement. Statistical analyses were performed using Python.

## 3 Results and discussion

### 3.1 Physiochemical and biological characteristics of the GoA during summertime

Sampling spanned from late spring (May) to the end of summer (September) within the euphotic zone (0–100 m) of the GoA. Surface temperatures ranged from  $\sim 25^\circ\text{C}$  in May to  $\sim 28^\circ\text{C}$  at the end of summer (September) and declined to  $\sim 23.5^\circ\text{C}$  at 100 m during all sampling events (Fig. 1A). Photosynthetic active radiation (PAR) levels ranged from  $\sim 1200$ – $1950 \mu\text{mol quanta m}^{-2} \text{ s}^{-1}$  at the surface and decreased exponentially to  $\sim 10$ – $20 \mu\text{mol quanta m}^{-2} \text{ s}^{-1}$  at 100 m (Fig. 1B), corresponding to 0.5 %–1.8 % of the surface irradiation levels. The corresponding diffuse attenuation coefficient ( $K_d$ ) was  $\sim 0.03$ – $0.04 \text{ m}^{-1}$ , in agreement with previous observations from the GoA (Dishon et al., 2012; Stambler, 2006) as well as in other oligotrophic regimes (Stambler, 2012). Concentrations of  $\text{NH}_4^+$  ranged from undetectable to  $65 \text{ nmol L}^{-1}$  (Fig. 1C). The corresponding integrated  $\text{NH}_4^+$  inventory (0–100 m) was lowest in May ( $1.68 \mu\text{mol m}^{-2}$ ) and highest in July ( $\sim 4.57 \mu\text{mol m}^{-2}$ ) (Table 1).  $\text{NO}_2^-$  levels were generally low throughout the upper 100 m (from below detection to  $< 20 \text{ nmol L}^{-1}$ ), except in September when nitrite increased with depth reaching  $\sim 45 \text{ nmol L}^{-1}$  below 40 m (Fig. 1D). Vertical  $\text{NO}_2^-$  profiles suggest active ammonia oxidation below the strongly lit surface waters, especially during September, although we cannot rule out expulsion of  $\text{NO}_2^-$  by phytoplankton under light limitation (Berube et al., 2023; Collos, 1998). The vertically integrated  $\text{NO}_2^-$  inventories ranged from 0.79– $3.39 \mu\text{mol m}^{-2}$  (Table 1). Surface  $\text{NO}_3^-$  was also low ( $< 20 \text{ nmol L}^{-1}$ ) and generally increased with depth, suggesting organic matter regeneration and nitrification during summertime (Fig. 1E), and/or that less  $\text{NO}_3^-$  is assimilated by phytoplankton at deeper depths. The integrated  $\text{NO}_3^-$  inventory ranged from  $2.65 \mu\text{mol m}^{-2}$  in May and September up to  $10.36 \mu\text{mol m}^{-2}$  in June (Table 1). Collectively, the summertime inorganic N species concentrations in the upper 100 m were low, in agreement with previous reports from the oligotrophic GoA (Mackey et al., 2011; Meeder et al., 2012; Rahav et al., 2015).

Chlorophyll-*a* concentrations were low in the surface water ( $< 0.15 \mu\text{g L}^{-1}$ ) and gradually increased with depth reaching maximal values in May and June ( $\sim 0.60 \mu\text{g L}^{-1}$ ) (Fig. 2A). The corresponding integrated chlorophyll-*a* was

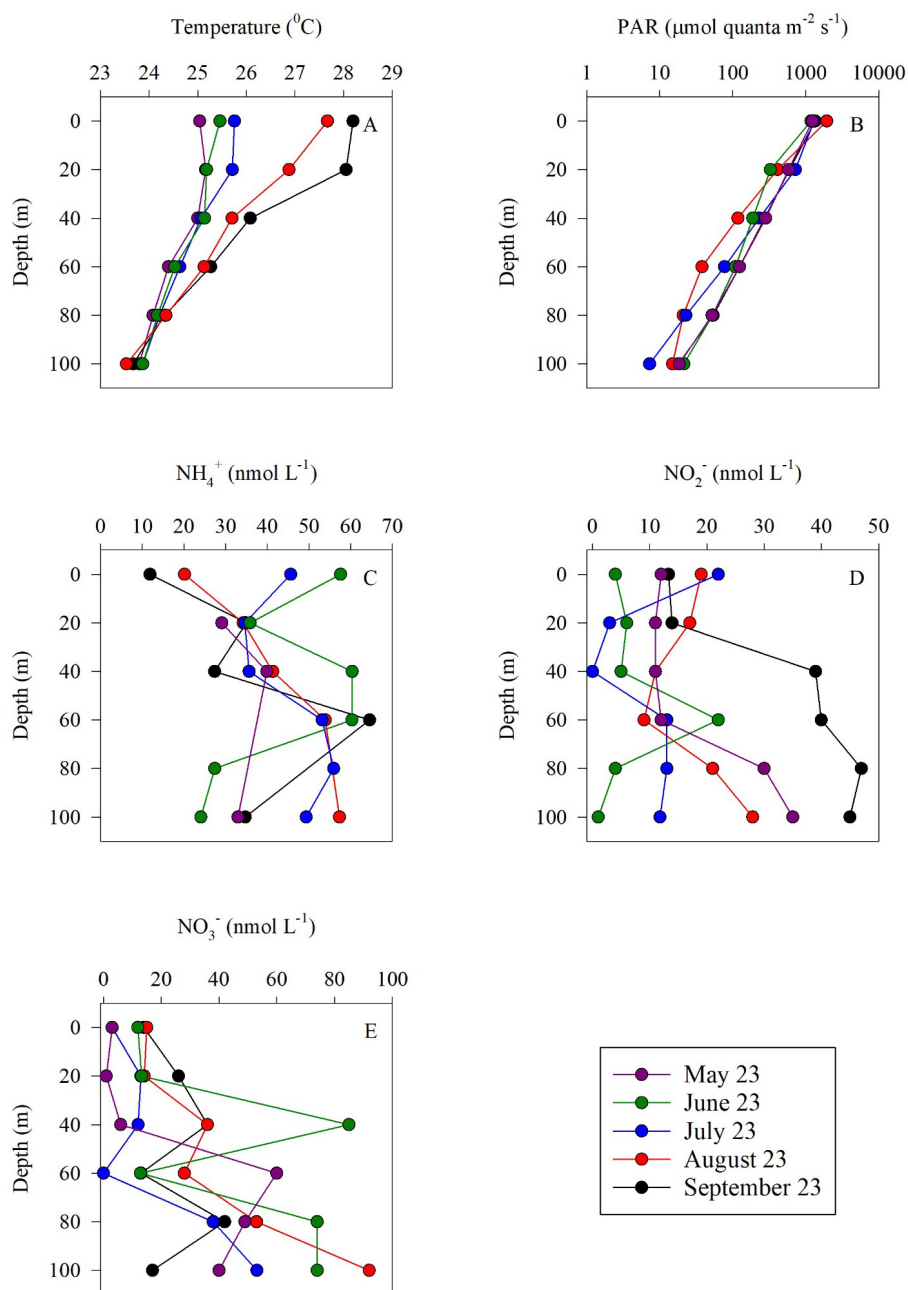


**Figure 1.** Vertical distribution of temperature (A), PAR (B),  $\text{NH}_4^+$  (C),  $\text{NO}_2^-$  (D) and  $\text{NO}_3^-$  (E) in the upper euphotic zone in the GoA, N Red Sea between May and September 2023.

$26\text{--}28\text{ mg m}^{-2}$  except in August where it was  $16\text{ mg m}^{-2}$  (Table 1). As expected, photosynthesis rates were highest in the surface water and decreased with depth (Fig. 2B), coinciding with the decreasing PAR levels (Fig. 1B). Photosynthesis rates decreased from  $\sim 10\text{ }\mu\text{g C L}^{-1}\text{ d}^{-1}$  at the surface to below detection at 100 m, except in September when elevated rates were observed throughout the water column, ranging from  $\sim 10\text{--}25\text{ }\mu\text{g C L}^{-1}\text{ d}^{-1}$  (Fig. 2B). The resulting integrated photosynthesis rates

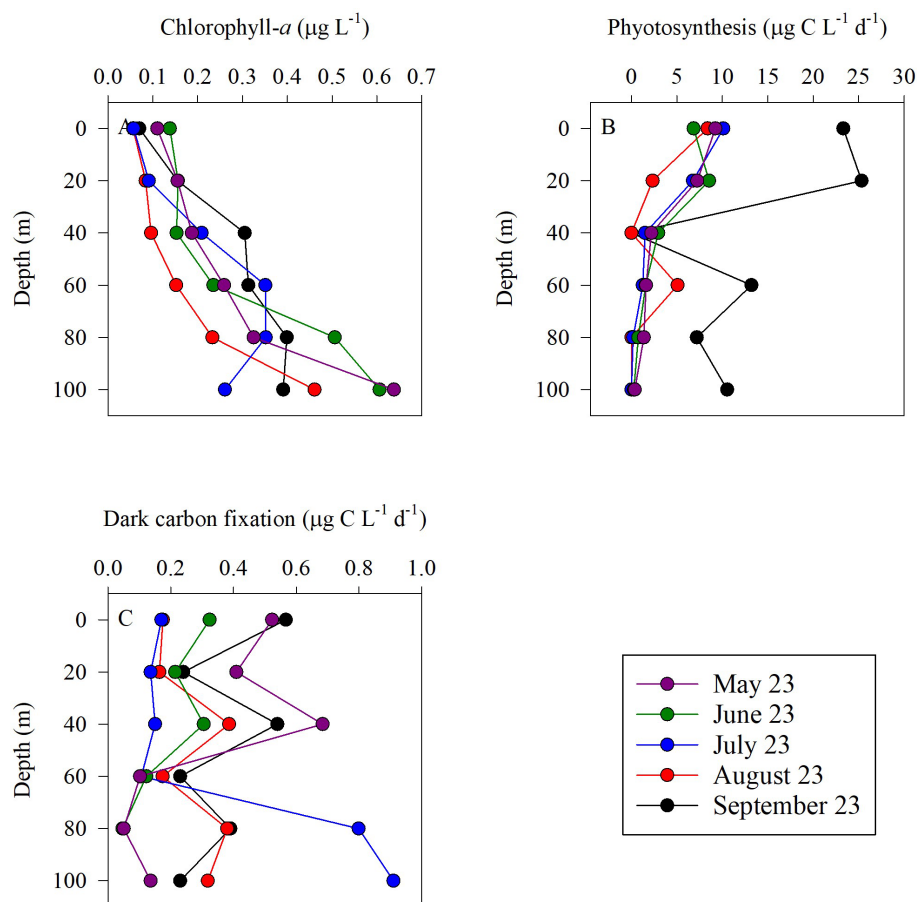
ranged from  $242\text{ mg C m}^{-2}\text{ d}^{-1}$  in August to as high as  $1263\text{ mg C m}^{-2}\text{ d}^{-1}$  in September (Table 1). Despite the fluctuation in photosynthetic rates between months, these values are within the range previously reported from the GoA (Rahav et al., 2015; Reich et al., 2024; Suggett et al., 2009).

Chemoautotrophic DCF was lower than photosynthesis rates and exhibited no clear vertical trends (Fig. 2C). The surface DCF ranged from  $\sim 0.2\text{--}0.6\text{ }\mu\text{g C L}^{-1}\text{ d}^{-1}$  to  $\sim 0.1\text{--}$

**Table 1.** Summary of integrated values (0–100 m) measured in the GoA (N Red Sea) during summer 2023.

Variable	23 May	23 June	23 July	23 August	23 September
Mixed layer depth (m) <sup>a</sup>	45	31	21	15	28
NH <sub>4</sub> <sup>+</sup> (μmol m <sup>-2</sup> )	1.68	4.54	4.57	3.36	2.99
NO <sub>2</sub> <sup>-</sup> (μmol m <sup>-2</sup> )	1.76	0.79	0.94	1.64	3.39
NO <sub>3</sub> <sup>-</sup> (μmol m <sup>-2</sup> )	2.76	10.36	6.60	6.13	2.65
Chlorophyll- <i>a</i> (mg m <sup>-2</sup> )	26	28	26	16	28
Photosynthesis (mg C m <sup>-2</sup> d <sup>-1</sup> )	350	349	302	242	1263
DCF (mg C m <sup>-2</sup> d <sup>-1</sup> )	32	17	35	27	37
NH <sub>4</sub> <sup>+</sup> oxidation (μmol m <sup>-2</sup> d <sup>-1</sup> )	28	48	39	45	56
NO <sub>2</sub> <sup>-</sup> oxidation (μmol m <sup>-2</sup> d <sup>-1</sup> )	24	38	45	39	44
Contribution of NH <sub>4</sub> <sup>+</sup> oxidation to DCF (%) <sup>b</sup>	0.32	1.02	0.40	0.60	0.54
Contribution of NO <sub>2</sub> <sup>-</sup> oxidation to DCF (%) <sup>c</sup>	0.05	0.13	0.08	0.09	0.07

<sup>a</sup> Calculated from a temperature threshold criterion ( $\Delta T = 0.2^\circ\text{C}$ ) from surface values (de Boyer Montégut et al., 2004). <sup>b</sup> Assuming 0.3 moles of C fixed per mole of NH<sub>4</sub><sup>+</sup> oxidized (Santoro et al., 2010). <sup>c</sup> Assuming 0.05 moles of C per mole of NO<sub>2</sub><sup>-</sup> oxidized (Beman et al., 2013).

**Figure 2.** Vertical distribution of chlorophyll-*a* (A), photosynthesis (B), and dark carbon fixation (C) in the upper euphotic zone in the GoA, N Red Sea between May and September 2023.

0.9 μg CL<sup>-1</sup> d<sup>-1</sup> at 100 m (Fig. 2C). The resulting integrated DCF ranged from 17–37 mg C m<sup>-2</sup> d<sup>-1</sup>, in agreement with a recent study from the GoA (Reich et al., 2024), corresponding to ~3%–10% of all the total autotrophic activity (photosynthesis and DCF combined). While multiple microbial

metabolisms involve chemoautotrophic carbon fixation, DCF is primarily attributed to ammonia and nitrite oxidation, as these chemoautotrophic metabolisms are ubiquitous throughout the oxic water column (Middelburg, 2011; Tang et al., 2023). In general, ammonia oxidation likely provides energy

that supports chemoautotrophic CO<sub>2</sub> assimilation throughout the euphotic zone. Though less energy efficient, nitrite oxidation also contributes to DCF and is considered especially relevant near the base of the euphotic zone where NO<sub>2</sub><sup>-</sup> often accumulates and reaches a maximum in concentration (Tang et al., 2023).

### 3.2 Ammonia and nitrite oxidation rates

Ammonia and nitrite oxidation rates were generally low throughout the euphotic zone yet exhibited an increasing trend with depth (Fig. 3), consistent with regulation by light inhibition. Overall, ammonia oxidation was homogeneous in the upper 40 m, ranging from ~0.10–0.55 nmol NL<sup>-1</sup> d<sup>-1</sup>. Below this depth rates increased towards the bottom of the euphotic zone (~100 m), ranging from ~0.26–0.83 nmol NL<sup>-1</sup> d<sup>-1</sup> (Fig. 3A and B). Ammonia oxidation rates often reached a maximum near the base of the euphotic zone (below the 50–100 m layer) as seen in other studies (reviewed by Tang et al., 2023). In general, these low euphotic zone ammonia oxidation rates are consistent with light inhibition, given the high PAR of the GoA during summer (Fig. 1B, Wan et al., 2021). Competition of nitrifiers with phytoplankton for NH<sub>4</sub><sup>+</sup> may also result in low ammonia oxidation rates, as has been reported in the surface sunlit North Pacific (Smith et al., 2014). However, the highest integrated ammonia oxidation rate (September, 56 μmol m<sup>-2</sup> d<sup>-1</sup>) was measured when chlorophyll-*a* levels and primary productivity were also relatively high and similar to springtime when the lowest ammonia oxidation rates were measured (May, 28 μmol m<sup>-2</sup> d<sup>-1</sup>) (Table 1). Thus, competition between nitrifiers and phytoplankton for NH<sub>4</sub><sup>+</sup> does not appear to play a direct role in the regulation of oxidation rates in our study. That said, the lack of correlation between chlorophyll *a* and ammonia ( $R^2 = 0.003$ ) does not preclude competition, but instead likely reflects rapid recycling and tight coupling between ammonium production and uptake. Ammonia oxidation rates have also been shown to be influenced by trace metal availability, specifically iron and copper (Martocello and Wankel, 2024; Shafiee et al., 2019, 2021). However, given the close proximity to major deserts, iron is not considered a limiting factor for microbes in the surface water of the GoA (Chen et al., 2008; Torfstein et al., 2017). The limiting factors for ammonia oxidizers in the GoA should be further studied by simulating different nutrients and temperature scenarios with or without amendments of an inhibitor of ammonia monooxygenase to better examine controls on environmental rates (Bayer et al., 2025).

During the study period, the mixed layer depth shoaled from ~45 m in May to ~15 m in August (Table 1), reflecting progressive seasonal stratification. The vertical pattern of ammonia oxidation (Fig. 3) suggests that rates remained low throughout the strongly illuminated upper water column, while modest increases at 60–80 m likely reflected reduced light inhibition and/or more favorable conditions for nitrifier

activity below the mixed layer. Thus, unlike systems where ammonia oxidation increases sharply below the deep chlorophyll maximum, nitrification in the GoA appears to follow a more gradual depth-related response during stratified conditions.

As with ammonia oxidation, rates of nitrite oxidation also increased with depth (Fig. 3C and D). Nitrite oxidation ranged from 0.14–0.70 nmol L<sup>-1</sup> d<sup>-1</sup> (Fig. 3C and D), with highest rates measured over 80–100 m. Integrated nitrite oxidation rates were lowest in spring/early summer (~24 μmol m<sup>-2</sup> d<sup>-1</sup>) and increased between June to September (38–45 μmol m<sup>-2</sup> d<sup>-1</sup>) (Table 1). Nitrite oxidation maxima (~100 m) were deeper than those of ammonia oxidation (~60 m). This vertical offset may reflect differences in substrate supply and the decoupling of ammonia and nitrite oxidation along the water column in addition to differential sensitivity to light (Wan et al., 2021). For example, ammonium supply may be more closely linked to shallower regeneration processes, whereas nitrite can accumulate and persist at greater depths (Travis et al., 2024). At the same time, near-zero ambient NO<sub>2</sub><sup>-</sup> or NO<sub>3</sub><sup>-</sup> at specific depths and months (e.g., 40 m for ammonia oxidation and 60 m for nitrite oxidation in July; Fig. 1) reflects extremely low product pool concentrations, which reduces the total N mass available for IRMS analysis. While this simultaneously reduces dilution of the <sup>15</sup>N-labelled product, resulting in elevated atom% enrichment, rate estimates at these depths carry greater analytical uncertainty and should be treated as conservative lower bounds on nitrification activity.

Our results demonstrate that ammonia and nitrite oxidation occurring at comparable rates, which is consistent with the typically low concentrations of NO<sub>2</sub><sup>-</sup> observed in the GoA during summertime (Fig. 1D, Meeder et al., 2012), and consistent with the low net accumulation of NO<sub>2</sub><sup>-</sup> resulting from limited decoupling between the two steps of nitrification. Converting photosynthesis to nitrogen demand using Redfield stoichiometry (C : N ≈ 6.6) suggests that phytoplankton nitrogen requirements in surface waters may substantially exceed the measured nitrification rates. This implies that regenerated nitrogen, including ammonium, is rapidly consumed, potentially limiting its availability for ammonia-oxidizing microorganisms. However, this inference is based on carbon-derived estimates of phytoplankton demand rather than direct measurements of nitrogen uptake and should therefore be interpreted cautiously. Nevertheless, previous studies indicate that ammonia uptake can greatly exceed nitrification rates in oligotrophic surface waters (Mackey et al., 2011).

To assess substrate control, we examined the relationship between NH<sub>4</sub><sup>+</sup> concentration and ammonia oxidation rates across depths. This relationship was weak overall (Pearson,  $r \approx 0.30$ ), whereas rates were more strongly associated with depth ( $r \approx 0.75$ ), indicating a dominant role of depth-related gradients (Fig. S1 in the Supplement and Table S1). When examined by depth intervals (0–50 m vs. 50–

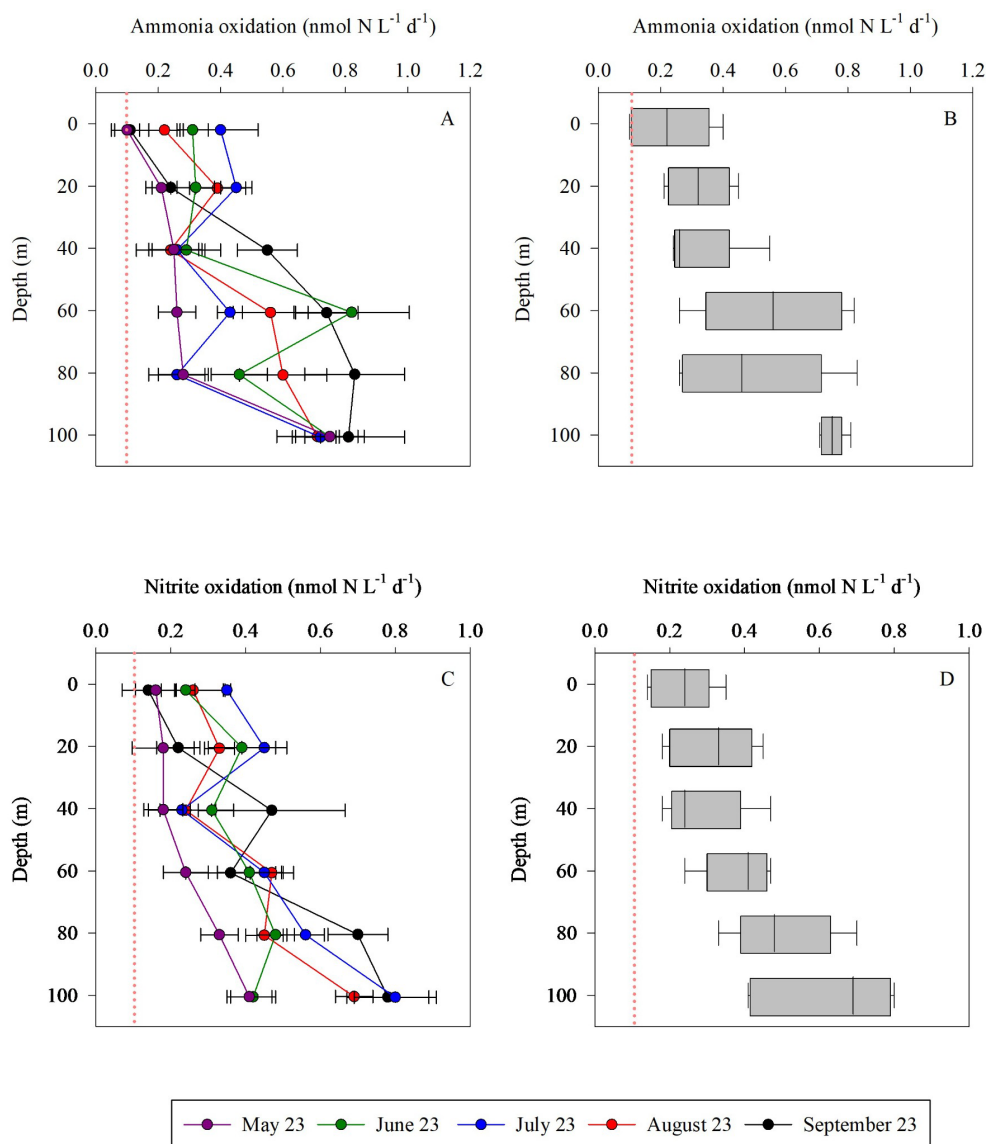


**Figure 3.** Vertical distribution of ammonia oxidation (A, B) and nitrite oxidation (C, D) in the upper euphotic zone in the GoA, N Red Sea between May and September 2023. The Box Whisker plots sum the data distribution per depth ( $n = 5$ ). The pink dashed line signifies the detection limit.

100 m), the  $\text{NH}_4^+$ -oxidation relationship was weak in the upper 50 m ( $r \approx 0.23$ ) and stronger  $> 50$  m ( $r \approx 0.41$ ) (Fig. S1, Table S1). This suggests that rapid recycling and competitive uptake weaken  $\text{NH}_4^+$ -oxidation rate coupling in surface waters, whereas reduced light inhibition at depth allows a somewhat greater influence of  $\text{NH}_4^+$ . These results are consistent with previous studies showing that nitrification maxima are often decoupled from  $\text{NH}_4^+$  peaks and instead reflect depth-dependent ecological structuring (Beman et al., 2012).

Note that a key consideration in interpreting the measured rates is the relative magnitude of the  $^{15}\text{NH}_4^+$  tracer addition compared to ambient substrate concentrations. In the upper euphotic zone, where  $\text{NH}_4^+$  concentrations were often

near detection limits (Fig. 1), the addition of  $\sim 20 \text{ nmol L}^{-1}$  (tracer) represented a substantial enrichment of the available pool. Under such conditions, if ammonia oxidation were strongly substrate-limited, one might expect a measurable stimulation of rates. However, the observed rates remained consistently low across depths and sampling periods (Table 1 and Fig. 3), even under these “enriched” conditions. This suggests that factors other than immediate substrate availability exert primary control over ammonia oxidation in the upper waters of the GoA. These may include low abundances of ammonia-oxidizing archaea (Aizawa et al., 2023; Smith et al., 2016), strong light inhibition in surface waters (Fig. 1B), or physiological constraints associated with

oligotrophic adaptation (Yin et al., 2024; Zhou et al., 2024). Rather than indicating the absence of substrate limitation per se, our results imply that ammonia oxidation operates under a combination of ecological and environmental constraints that limit its overall contribution to nitrogen cycling in this system. Moreover, the use of 24 h incubations introduce additional uncertainty, as internal recycling of ammonium and microbial interactions may partially decouple measured rates from instantaneous *in situ* conditions. Therefore, the rates reported here are interpreted as conservative estimates of nitrification potential in the upper euphotic zone. Adding to that, in oligotrophic systems, rapid recycling of dissolved inorganic nitrogen can influence both substrate availability (Christie-Oleza et al., 2017) and isotopic enrichment during incubation experiments (Stukel, 2020). Thus, processes such as ammonium regeneration and microbial uptake may dilute the  $^{15}\text{N}$  substrate pool or reduce accumulation of labelled products (Braun et al., 2018). However, we surmise that any such processes, if occurred here, would tend to reduce the apparent isotopic enrichment and thus bias rate estimates toward underestimation. Another possible limitation regards the uncertainty in low nutrient concentrations in the GoA (most notably within the upper mixed layer depth) that may propagate into rate calculations, as substrate concentrations are explicitly included in the rate equations (see equations 1–3). However, such uncertainty affects absolute rate estimates proportionally and does not alter the overall interpretation of low nitrification activity. Accordingly, the reported rates should be considered conservative estimates of nitrification activity over the incubation period. Future work in similar ultra-oligotrophic settings could benefit from newer low-concentration nitrate and nitrite isotope protocols (e.g., Jiang et al., 2026), which explicitly target sub nanomolar N species.

### 3.3 Contribution of ammonia and nitrite oxidation to DCF

DCF is widely thought to be dominated by ammonia and nitrite oxidation, as these metabolic processes provide energy that, in turn, support chemoautotrophic  $\text{CO}_2$  assimilation (Middelburg, 2011), although additional pathways such as urea oxidation by ammonia oxidizers may also contribute (Wan et al., 2024). While other chemoautotrophic metabolisms, such as sulfur oxidation, anammox or methanotrophy also represent important drivers of chemoautotrophy in some environments, these are unlikely to be relevant in the oxic, oligotrophic waters of the GoA. DCF and nitrification are rarely measured simultaneously, which prevents robust assessment of this relationship. Here, we explored DCF under the warm, high-light, nutrient-poor conditions found in the GoA (Fig. 1) and investigated how it relates to corresponding rates of nitrification over the euphotic zone. We calculated the contribution of ammonia and nitrite oxidation to DCF assuming 0.3 moles of C fixed per mole of  $\text{NH}_4^+$  (San-

toro et al., 2010). Overall, the depth-integrated contribution of ammonia oxidation to DCF ranged between 0 %–2 %, consistent, yet often lower than reports from other oceanographic settings. For example, ammonia oxidizers contributed only a small fraction to DCF in the eastern tropical Pacific, accounting for < 20 % of depth-integrated rates (Bayer et al., 2025). The depth-integrated contribution of nitrite oxidation to DCF was negligible, accounting for 0.05 %–0.13 % (Table 1). Thus, ammonia and nitrite oxidation together could account for only  $\sim 1$  % of the DCF, lower than recent estimates from the eastern tropical Pacific (Bayer et al., 2025), though similar to observations in culture experiments with ammonia oxidizers (Bayer et al., 2023). It is notable, however, that relevant conversion factors between moles C fixed per mole of N oxidized in the ocean should be better constrained (and may be site-specific) (Tang et al., 2023), which could alter the calculated contribution discussed here. Nevertheless, we show that ammonia and nitrite oxidation link N recycling with inorganic carbon assimilation in the euphotic zone in the GoA, and while their contribution to total primary production is relatively small, it may sustain part of the microbial metabolism in the nutrient-depleted surface waters of the GoA. Our results suggest that other microbial metabolism processes (e.g., anaplerosis) may also contribute to DCF in the GoA's euphotic zone and should be estimated separately in future studies.

DCF in the sunlit ocean should not be interpreted solely as nitrification-driven chemoautotrophy. Even under dark incubation conditions, inorganic carbon fixation may include contributions from phytoplankton-associated dark metabolism, heterotrophic inorganic carbon assimilation, and other microbial pathways (Baltar and Herndl, 2019; Reich et al., 2026). A recent 10 year analysis from the GoA (same study site) showed that DCF is a persistent but variable component of carbon cycling, contributing substantially to total autotrophic carbon fixation (Reich et al., 2024). Therefore, while our data suggests that ammonia and nitrite oxidation contribute only a minor fraction of total DCF, the remaining DCF signal likely reflects multiple unresolved microbial processes (Reich et al., 2025).

### 3.4 Environmental drivers affecting ammonia and nitrite oxidation

Nitrification is known to be affected by PAR, oxygen levels, temperature, nitrogen substrate availability, pH, as well as by other environmental factors (Ward, 2008). Our results are consistent overall with previous observations at other sites as both ammonia and nitrite oxidation rates linearly correlate with most of these environmental variables, either positively or negatively (Figs. 4, S1 and Tables S1 and S2). Most notably, ammonia and nitrite oxidation rates correlated with increasing depth and decreasing PAR level, consistent with previous reports showing that light inhibit nitrifier growth and nitrification rates (Merbt et al., 2012; Olsen, 1989; Xu

et al., 2019). Temperature correlated negatively with ammonia and nitrite oxidation rates (Fig. 4,  $r = 0.61$ ,  $p < 0.01$ ), likely reflects substrate limitation rather than a direct temperature effect. Previous studies showed that increasing temperature generally stimulates nitrification by simultaneously altering substrate availability and enzyme kinetics (Emerson et al., 1975). As temperature increases, the pKa of the  $\text{NH}_4^+$ – $\text{NH}_3$  system decreases, shifting the equilibrium toward  $\text{NH}_3$ , the putative substrate of ammonia monooxygenase (Emerson et al., 1975). In parallel, warming enhances enzymatic activity, accelerating the catalytic steps of both ammonia and nitrite oxidation (Zheng et al., 2017, 2020). We surmise that in the stratified GoA, warming strengthened stratification, enhanced photo-inhibition, and thereby increased biological competition for ammonium, thus reducing substrate supply to nitrifiers despite favorable enzyme kinetics, leading to the observed negative correlation between temperature and nitrification. In agreement with this line of thought, substrate availability was positively correlated with ammonia oxidation ( $\text{NH}_4^+$ ,  $\text{NO}_2^-$ ) and nitrite oxidation ( $\text{NO}_2^-$ ,  $\text{NO}_3^-$ ), highlighting the substrate-dependent nature of nitrification. Alternatively, these relationships may reflect co-variation with depth and associated environmental gradients, rather than direct substrate control alone (discussed below). Ammonia oxidation requires  $\text{NH}_4^+$  or  $\text{NH}_3$  as the electron donor, while nitrite oxidation depends on  $\text{NO}_2^-$  availability. Elevated ambient concentrations of these substrates make them more available to nitrifying enzymes, resulting in higher reaction rates until enzymatic saturation or co-limitation with other nutrients are reached (e.g., vitamins and other co-factors,  $\text{PO}_4^+$ ). In oligotrophic systems such as the GoA, where ambient  $\text{NH}_4^+$  and  $\text{NO}_2^-$  concentrations are exceptionally low, even small pulses of reduced or intermediate nitrogen (e.g., from organic matter remineralization, mixing, or atmospheric deposition) may trigger an increase in nitrification rates.

Nitrification is generally expected to show a negative relationship with chlorophyll-*a* in surface waters, where phytoplankton may compete with nitrifiers for reduced nitrogen species. Consequently, most studies report suppressed ammonia and nitrite oxidation rates near the surface and enhanced rates below the chlorophyll maximum once light levels decrease and substrate regeneration through organic matter remineralization becomes more important (Beman et al., 2013; Yool et al., 2007). Here, however, we observed a positive correlation between chlorophyll-*a* and ammonia or nitrite oxidation (as well as with photosynthesis, although not significantly). This pattern likely reflects conditions near the deep chlorophyll maximum (~80–100 m), where chlorophyll-*a* is elevated due to photo-acclimation under low light conditions rather than strictly higher biomass (Cornec et al., 2021; Fennel and Boss, 2003; Scofield et al., 2020). In these depths, reduced irradiance and enhanced organic matter turnover may promote ammonium regeneration, providing substrate that supports nitrification. These findings suggest that the expected negative coupling at the surface is

offset by strong regeneration and oxidation processes near the deep chlorophyll maxima, resulting in an overall positive relationship when integrated across the euphotic zone.

We expected that ammonia and nitrite oxidation would show a significant correlation with DCF (see discussion above). Nevertheless, although both ammonia and nitrite oxidation were positively coupled with DCF ( $r = 0.49$  and  $0.17$ , respectively), the correlations were not statistically significant ( $p > 0.05$ ) and is in line with the overall low contribution of these processes to DCF (discussion above and see Table 1). This suggests that additional pathways such as anaerobic processes may contribute to DCF (Dijkhuizen and Harder, 1984; Erb, 2011), as well as other chemoautotrophic metabolisms beyond nitrification such as urea oxidation, sulfur oxidation and iron oxidation (Arandia-Gorostidi et al., 2024; Dang and Chen, 2017), while the contribution of ammonia and nitrite oxidation to total DCF is low (Table 1).

We note that correlation analysis should be interpreted with caution. Many parameters considered here co-vary with depth (e.g., PAR, chlorophyll-*a*) and seasonal stratification (mixed layer depth), which can produce strong apparent relationships without implying direct mechanistic coupling. Furthermore, as the dataset is restricted to the upper 100 m, it does not capture the full vertical structure of nitrification, including deeper maxima often observed below the deep chlorophyll maximum. Accordingly, these correlations primarily reflect processes operating within the upper euphotic zone and should not be extrapolated beyond this depth range. Lastly, while variations in ammonia oxidation rates broadly co-occurred with changes in primary production and chlorophyll-*a*, these relationships should be interpreted with caution. In this study, phytoplankton activity was assessed using carbon-based proxies, and no direct measurements of nitrogen uptake or community composition were conducted. Therefore, any inferred coupling between phytoplankton dynamics and nitrification remains indirect. The observed patterns are consistent with the expectation that phytoplankton influence the availability and cycling of regenerated nitrogen, but do not allow us to disentangle the relative roles of substrate competition, regeneration, or microbial community structure. Future studies that combine measurements of phytoplankton nitrogen demand, ammonium regeneration, and nitrifier abundance and activity will be required to directly resolve these interactions in oligotrophic systems.

## 4 Conclusions

Globally, ammonia and nitrite oxidation rates in the euphotic zone span several orders of magnitude across offshore oceanic environments (Tang et al., 2023, Fig. 5). The rates we measured in the GoA during summer fall below the global median (i.e., the red vs. black lines in Fig. 5). The reason for the low rates in GoA is attributed to the low substrate

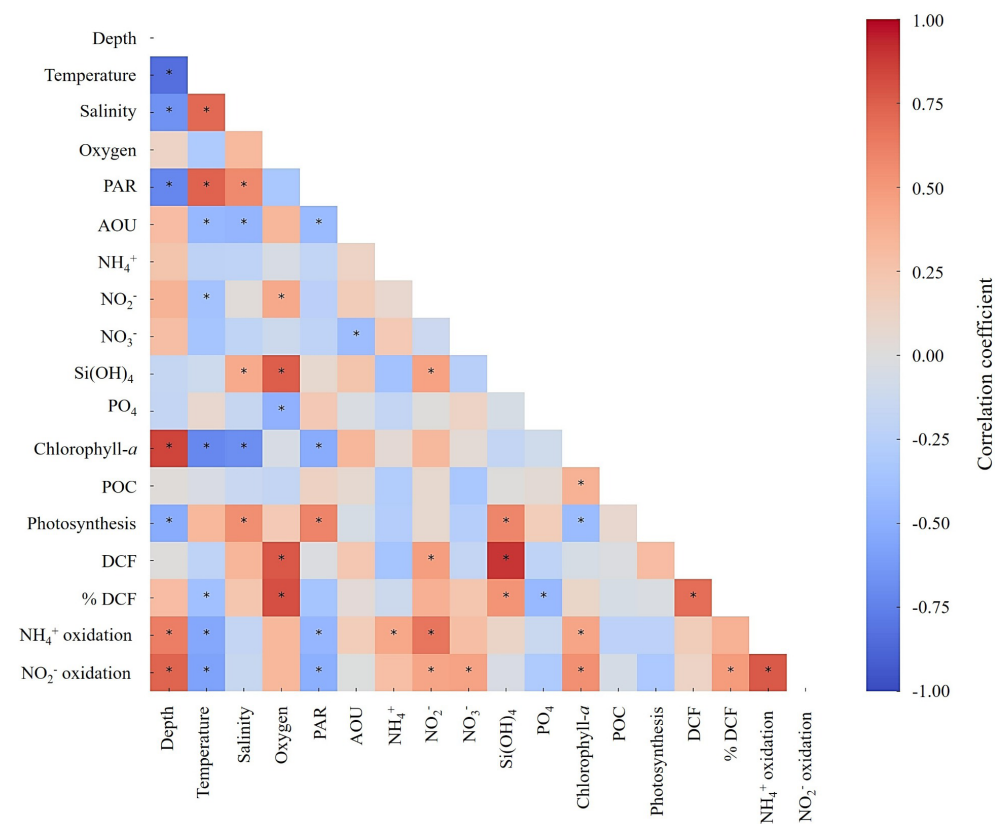


**Figure 4.** A heatmap showing Pearson correlation coefficients among measured environmental parameters and biogeochemical rates. Color shading indicates the strength and direction of the correlation. Asterisks denote statistically significant correlations ( $p < 0.05$ ). Full descriptive statistics for the correlations are provided in Tables S1 and S2.

availability during summertime (Fig. 1C–E) but likely reflect a combination of environmental and ecological constraints rather than a single controlling factor. For example, the combination of high light intensity (Fig. 1B) and penetration (i.e.,  $K_d \approx 0.04 \text{ m}^{-1}$ ) and enhanced stratification (Fig. 1A) can further suppress nitrifier activity, either through photoinhibition of ammonia monooxygenase and/or by pushing microbial communities closer to their thermal tolerance limits. Moreover, the absence of measurements of nitrifier abundance preclude us from distinguishing whether low bulk rates reflect low population size or potentially high per-cell activity.

Additionally, while our results suggest a potential linkage between phytoplankton activity and nitrogen cycling, this inference is based on carbon-derived proxies (primary production and chlorophyll-*a*) rather than direct measurements of species-specific nitrogen uptake or microbial community composition using genetic markers. Resolving this coupling will require future studies that simultaneously quantify phytoplankton nitrogen demand, ammonium regeneration, and nitrifier abundance and activity.

Future studies should focus on resolving the temporal and spatial variability of nitrification rates and nitrifier com-

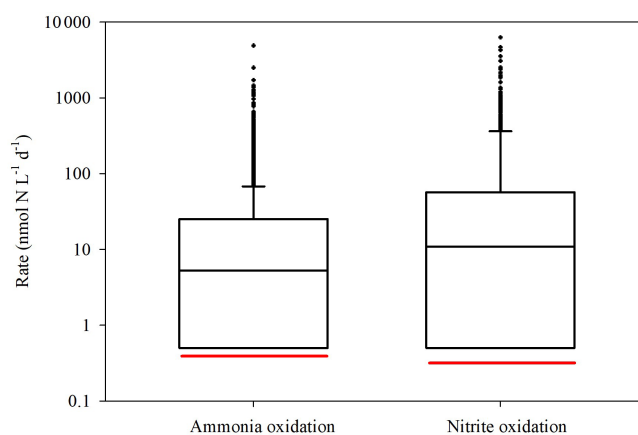


**Figure 5.** A literature compilation of reported euphotic zone's ammonia oxidation and nitrite oxidation recently reviewed Tang et al. (2023) and this study. The black line inside the boxes shows the median value of all studies considered, while the red line indicates the median values measured in the GoA during this study. Data include only offshore euphotic-zone measurements as defined in the original studies. We note that the depth and definition of the euphotic zone vary among regions, which may contribute to variability in reported rates.

munities in the context of ongoing climate change. This is especially true for the GoA that experience rapid warming and ocean acidification. Long-term time series and diel-scale observations are needed to capture seasonal, interannual, and daily dynamics, particularly in relation to stratification, warming, and nutrient supply. Advanced molecular approaches such as metagenomics, metatranscriptomics, and single-cell tools should be applied to link community composition and functional potential with in-situ rate measurements. Parallel measurements of trace metals will be essential to assess their role as cofactors or inhibitors of key enzymes in ammonia and nitrite oxidation. Furthermore, the contribution of nitrification to DCF appears to be limited, suggesting that additional microbial pathways contribute to inorganic carbon fixation in this system. Constraining these contributions will require future studies that integrate rate measurements with microbial community and metabolic analyses to better resolve the sources of DCF in oligotrophic waters. Ultimately, combining high-resolution field observations with targeted manipulations and modelling will improve our ability to predict how nitrification responds to environmental change and contributes to current and future ocean nitrogen cycling.

*Data availability.* All the data is presented in the graphs/table/text and will be made available in excel format upon request.

*Supplement.* The supplement related to this article is available online at <https://doi.org/10.5194/bg-23-4171-2026-supplement>.

*Author contributions.* Conceptualized and conducted the field measurements; ER. Data curation, formal analysis, and visualization; ER, SDW and AP. The paper was prepared by ER, SDW and AP.

*Competing interests.* The contact author has declared that none of the authors has any competing interests.

*Disclaimer.* Publisher's note: Copernicus Publications remains neutral with regard to jurisdictional claims made in the text, published maps, institutional affiliations, or any other geographical representation in this paper. The authors bear the ultimate responsibility for providing appropriate place names. Views expressed in the text are those of the authors and do not necessarily reflect the views of the publisher.

*Acknowledgements.* The authors thank the personnel in the Inter University Institute for Marine Sciences in Eilat (IUI). We also thank the two anonymous reviewers for their constructive comments, which helped to significantly improve and refine the manuscript.

*Financial support.* This paper was supported by a grant from the Middle East Regional Cooperation (MERC) (M39-011) to Eyal Rahav and Adina Paytan.

*Review statement.* This paper was edited by Yuan Shen and reviewed by two anonymous referees.

## References

- Aizawa, A., Watanabe, Y., Hashioka, K., Kadoya, A., Suzuki, S., Yoshimura, T., and Kudo, I.: Contribution of ammonium oxidizing archaea and bacteria to intensive nitrification during summer in Mutsu Bay, Japan, *Reg. Stud. Mar. Sci.*, 63, 102984, <https://doi.org/10.1016/j.rsma.2023.102984>, 2023.
- Arandia-Gorostidi, N., Jaffe, A. L., Parada, A. E., Kapili, B. J., Casciotti, K. L., Salcedo, R. S. R., Baumas, C. M. J., and Dekas, A. E.: Urea assimilation and oxidation support activity of phylogenetically diverse microbial communities of the dark ocean, *ISME J.*, 18, <https://doi.org/10.1093/ismejo/wrae230>, 2024.
- Baltar, F. and Herndl, G. J.: Ideas and perspectives: Is dark carbon fixation relevant for oceanic primary production estimates?, *Biogeosciences*, 16, 3793–3799, <https://doi.org/10.5194/bg-16-3793-2019>, 2019.
- Bayer, B., McBeain, K., Carlson, C. A., and Santoro, A. E.: Carbon content, carbon fixation yield and dissolved organic carbon release from diverse marine nitrifiers, *Limnol. Oceanogr.*, 68, 84–96, <https://doi.org/10.1002/lno.12252>, 2023.
- Bayer, B., Kitzinger, K., Paul, N. L., Albers, J. B., Saito, M. A., Wagner, M., Carlson, C. A., and Santoro, A. E.: Minor contribution of ammonia oxidizers to inorganic carbon fixation in the ocean, *Nat. Geosci.*, 18, 1144–1151, <https://doi.org/10.1038/s41561-025-01798-x>, 2025.
- Belkin, N., Guy-Haim, T., Rubin-Blum, M., Lazar, A., Sisma-Ventura, G., Kiko, R., Morov, A. R., Ozer, T., Gertman, I., Herut, B., and Rahav, E.: Influence of cyclonic and anticyclonic eddies on plankton in the southeastern Mediterranean Sea during late summertime, *Ocean Sci.*, 18, 693–715, <https://doi.org/10.5194/os-18-693-2022>, 2022.
- Beman, J. M., Chow, C.-E., King, A. L., Feng, Y., Fuhrman, J. A., Andersson, A., Bates, N. R., Popp, B. N., and Hutchins, D. A.: Global declines in oceanic nitrification rates as a consequence of ocean acidification, *P. Natl. Acad. Sci. USA*, 108, 208–213, <https://doi.org/10.1073/pnas.1011053108>, 2011.
- Beman, J. M., Leilei Shih, J., and Popp, B. N.: Nitrite oxidation in the upper water column and oxygen minimum zone of the eastern tropical North Pacific Ocean, *ISME J.*, 7, 2192–2205, <https://doi.org/10.1038/ismej.2013.96>, 2013.
- Berube P. M., O'Keefe T. J., Rasmussen, A., LeMaster, T., and Chisholm, S. W.: Production and cross-feeding of nitrite within *Prochlorococcus* populations, *mBio*, 14, e01236-23, <https://doi.org/10.1128/mbio.01236-23>, 2023.
- de Boyer Montégut, C., Madec, G., Fischer, A. S., Lazar, A., and Iudicone, D.: Mixed layer depth over the global ocean: An examination of profile data and a profile-based climatology, *J. Geophys. Res.-Ocean.*, 109, C12003, <https://doi.org/10.1029/2004JC002378>, 2004.

- Braun, J., Mooshammer, M., Wanek, W., Prommer, J., Walker, T. W. N., Rütting, T., and Richter, A.: Full  $^{15}\text{N}$  tracer accounting to revisit major assumptions of  $^{15}\text{N}$  isotope pool dilution approaches for gross nitrogen mineralization, *Soil Biol. Biochem.*, 117, 16–26, <https://doi.org/10.1016/j.soilbio.2017.11.005>, 2018.
- Bristow, L. A., Sarode, N., Cartee, J., Caro-Quintero, A., Thamdrupe, B., and Stewart, F. J.: Biogeochemical and metagenomic analysis of nitrite accumulation in the Gulf of Mexico hypoxic zone, *Limnol. Oceanogr.*, 60, 1733–1750, <https://doi.org/10.1002/lno.10130>, 2015.
- Casciotti, K. L., Sigman, D. M., Hastings, M. G., Böhlke, J. K., and Hilkert, A.: Measurement of the oxygen isotopic composition of nitrate in seawater and freshwater using the denitrifier method., *Anal. Chem.*, 74, 4905–4912, <https://doi.org/10.1021/ac020113w>, 2002.
- Chen, Y., Paytan, A., Chase, Z., Measures, C., Beck, A. J., Sañudo-Wilhelmy, S. A., and Post, A. F.: Sources and fluxes of atmospheric trace elements to the Gulf of Aqaba, Red Sea, *J. Geophys. Res.-Atmos.*, 113, 1–13, <https://doi.org/10.1029/2007JD009110>, 2008.
- Christie-Oleza, J. A., Sousoni, D., Lloyd, M., Armengaud, J., and Scanlan, D. J.: Nutrient recycling facilitates long-term stability of marine microbial phototroph-heterotroph interactions, *Nat. Microbiol.*, 2, 17100, <https://doi.org/10.1038/nmicrobiol.2017.100>, 2017.
- Clark, D. R., Rees, A. P., and Joint, I.: Ammonium regeneration and nitrification rates in the oligotrophic Atlantic Ocean: Implications for new production estimates, *Limnol. Oceanogr.*, 53, 52–62, <https://doi.org/10.4319/lo.2008.53.1.0052>, 2008.
- Clark, D. R., Rees, A. P., Ferrera, C. M., Al-Moosawi, L., Somerfield, P. J., Harris, C., Quartly, G. D., Goult, S., Tarran, G., and Lessin, G.: Nitrite regeneration in the oligotrophic Atlantic Ocean, *Biogeosciences*, 19, 1355–1376, <https://doi.org/10.5194/bg-19-1355-2022>, 2022.
- Collos, Y.: Nitrate uptake, nitrite release and uptake, and new production estimates, *Mar. Ecol. Prog. Ser.*, 171, 293–301, 1998.
- Cornec, M., Claustre, H., Mignot, A., Guidi, L., Lacour, L., Poteau, A., D’Ortenzio, F., Gentili, B., and Schmechtig, C.: Deep chlorophyll maxima in the global ocean: occurrences, drivers and characteristics, *Global Biochem. Cy.*, 35, e2020GB006759, <https://doi.org/10.1029/2020GB006759>, 2021.
- Daims, H., Lebedeva, E. V., Pjevac, P., Han, P., Herbold, C., Albertsen, M., Jehmlich, N., Palatinszky, M., Vierheilig, J., Bulaev, A., Kirkegaard, R. H., von Bergen, M., Rattei, T., Bendinger, B., Nielsen, P. H., and Wagner, M.: Complete nitrification by *Nitrospira* bacteria, *Nature*, 528, 504–509, <https://doi.org/10.1038/nature16461>, 2015.
- Dang, H. and Chen, C.-T. A.: Ecological energetic perspectives on responses of nitrogen-transforming chemolithoautotrophic microbiota to changes in the marine environment, *Front. Microbiol.*, 8, 1246, <https://doi.org/10.3389/fmicb.2017.01246>, 2017.
- Dijkhuizen, L. and Harder, W.: Current views on the regulation of autotrophic carbon dioxide fixation via the Calvin cycle in bacteria, *Antonie Van Leeuwenhoek*, 50, 473–487, <https://doi.org/10.1007/BF02386221>, 1984.
- Dishon, G., Dubinsky, Z., Caras, T., Rahav, E., Bar-Zeev, E., Tzuber, Y., and Iluz, D.: Optical habitats of ultraphytoplankton groups in the Gulf of Eilat (Aqaba), Northern Red Sea, *Int. J. Remote Sens.*, 33, 2683–2705, <https://doi.org/10.1080/01431161.2011.619209>, 2012.
- Dodds, W. K. and Jones, R. D.: Potential rates of nitrification and denitrification in an oligotrophic freshwater sediment system, *Microb. Ecol.*, 14, 91–100, 1987.
- Emerson, K., Russo, R. C., Lund, R. E., and Thurston, R. V.: Aqueous ammonia equilibrium calculations: effect of pH and temperature, *J. Fish. Res. Board Can.*, 32, 2379–2383, <https://doi.org/10.1139/f75-274>, 1975.
- Eppley, R. W. and Peterson, B. J.: Particulate organic matter flux and planktonic new production in the deep ocean, *Nature*, 282, 677–680, <https://doi.org/10.1038/282677a0>, 1979.
- Erb, T. J.: Carboxylases in Natural and Synthetic Microbial Pathways, *Appl. Environ. Microb.*, 77, <https://doi.org/10.1128/AEM.05702-11>, 2011.
- Fawcett, S. E., Lomas, M. W., Casey, J. R., Ward, B. B., and Sigman, D. M.: Assimilation of upwelled nitrate by small eukaryotes in the Sargasso Sea, *Nat. Geosci.*, 4, 717–722, <https://doi.org/10.1038/ngeo1265>, 2011.
- Fei, X., Jian-Gong, W., Ting, Z., Bin, Z., Sung-Keun, R., and Zhe-Xue, Q.: Ubiquity and diversity of complete ammonia oxidizers (Comammox), *Appl. Environ. Microb.*, 84, e01390-18, <https://doi.org/10.1128/AEM.01390-18>, 2018.
- Fennel, K. and Boss, E.: Subsurface maxima of phytoplankton and chlorophyll: Steady-state solutions from a simple model, *Limnol. Oceanogr.*, 48, 1521–1534, <https://doi.org/10.4319/lo.2003.48.4.1521>, 2003.
- Francis, C. A., Roberts, K. J., Beman, J. M., Santoro, A. E., and Oakley, B. B.: Ubiquity and diversity of ammonia-oxidizing archaea in water columns and sediments of the ocean, *P. Natl. Acad. Sci. USA*, 102, 14683–14688, <https://doi.org/10.1073/pnas.0506625102>, 2005.
- Fuller, N. J., West, N. J., Marie, D., Yallop, M., Rivlin, T., Post, A. F., Interuniversity, T., Sciences, M., Beach, C., and Scanlan, D. J.: Dynamics of community structure and phosphate status of picocyanobacterial populations in the Gulf of Aqaba, Red Sea, 50, 363–375, 2005.
- Granger, J. and Sigman, D. M.: Removal of nitrite with sulfamic acid for nitrate N and O isotope analysis with the denitrifier method, *Rapid Commun. Mass Sp.*, 23, 3753–3762, <https://doi.org/10.1002/rcm.4307>, 2009.
- Grasshoff, K., Kremling, K., and Ehrhardt, M.: Methods of seawater analysis, 3rd edn., edited by: Kremling, K., Ehrenreich, I. M., and Grasshoff, K., Wiley, New York, 632 pp., ISBN: 978-3-527-61399-1, 1999.
- Henriksen, K. and Kemp, W. M.: Nitrification in estuarine and coastal marine sediments, in: *Nitrogen Cycling in Coastal Marine Environments*, edited by: Blackburn, T. and Sorensen, J., John Wiley & Sons, Ltd, 207–249, ISBN: 978-0-471-91404-4, 1988.
- Herbert, R. A.: Nitrogen cycling in coastal marine ecosystems, *FEMS Microbiol. Rev.*, 23, 563–590, <https://doi.org/10.1111/j.1574-6976.1999.tb00414.x>, 1999.
- Holms, R., Aminot, A., Kérouel, R., Hooker, B., and Peterson, B.: A simple and precise method for measuring ammonium in marine and freshwater ecosystems, *Can. Data Rep. Fish. Aquat. Sci.*, 56, 1801–1808, <https://doi.org/10.1139/cjfas-56-10-1801>, 1999.
- Jiang, M., Koba, K., Ono, M., and Hayashi, K.: Improved isotopic analysis of low-concentration freshwater nitrite by anion-

- exchange resin enrichment and azide reduction, *Anal. Chem.*, 98, 2956–2967, <https://doi.org/10.1021/acs.analchem.5c05937>, 2026.
- van Kessel, M. A. H. J., Speth, D. R., Albertsen, M., Nielsen, P. H., Op den Camp, H. J. M., Kartal, B., Jetten, M. S. M., and Lücker, S.: Complete nitrification by a single microorganism, *Nature*, 528, 555–559, <https://doi.org/10.1038/nature16459>, 2015.
- Mackey, K. R. M., Labiosa, R. G., Calhoun, M., Street, J. H., Post, A. F., and Paytan, A.: Phosphorus availability, phytoplankton community dynamics, and taxon-specific phosphorus status in the Gulf of Aqaba, Red Sea, *Limnol. Oceanogr.*, 52, 873–885, <https://doi.org/10.4319/lo.2007.52.2.0873>, 2007.
- Mackey, K. R. M., Bristow, L., Parks, D. R., Altabet, M. A., Post, A. F., and Paytan, A.: The influence of light on nitrogen cycling and the primary nitrite maximum in a seasonally stratified sea, *Prog. Oceanogr.*, 91, 545–560, <https://doi.org/10.1016/j.pocean.2011.09.001>, 2011.
- Martocello, D. E. and Wankel, S. D.: Physiological influence of Fe and Cu availability on nitrogen isotope fractionation during ammonia oxidation, *Environ. Sci. Technol.*, 58, 421–431, <https://doi.org/10.1021/acs.est.3c05964>, 2024.
- McIlvin, M. R. and Altabet, M. A.: Chemical conversion of nitrate and nitrite to nitrous oxide for nitrogen and oxygen isotopic analysis in freshwater and seawater, *Anal. Chem.*, 77, 5589–5595, <https://doi.org/10.1021/ac050528s>, 2005.
- McIlvin, M. R. and Casciotti, K. L.: Technical updates to the bacterial method for nitrate isotopic analyses, *Anal. Chem.*, 83, 1850–1856, <https://doi.org/10.1021/ac1028984>, 2011.
- Mdutyana, M., Thomalla, S. J., Philibert, R., Ward, B. B., and Fawcett, S. E.: The seasonal cycle of nitrogen uptake and nitrification in the Atlantic sector of the Southern Ocean, *Global Biogeochem. Cy.*, 34, e2019GB006363, <https://doi.org/10.1029/2019GB006363>, 2020.
- Meeder, E., MacKey, K. R. M., Paytan, A., Shaked, Y., Iluz, D., Stambler, N., Rivlin, T., Post, A. F., and Lazar, B.: Nitrite dynamics in the open ocean-clues from seasonal and diurnal variations, *Mar. Ecol. Prog. Ser.*, 453, 11–26, <https://doi.org/10.3354/meps09525>, 2012.
- Merbt, S. N., Stahl, D. A., Casamayor, E. O., Martí, E., Nicol, G. W., and Prosser, J. I.: Differential photoinhibition of bacterial and archaeal ammonia oxidation, *FEMS Microbiol. Lett.*, 327, 41–46, <https://doi.org/10.1111/j.1574-6968.2011.02457.x>, 2012.
- Michael Beman, J., Popp, B. N., and Alford, S. E.: Quantification of ammonia oxidation rates and ammonia-oxidizing archaea and bacteria at high resolution in the Gulf of California and eastern tropical North Pacific Ocean, *Limnol. Oceanogr.*, 57, 711–726, <https://doi.org/10.4319/lo.2012.57.3.0711>, 2012.
- Middelburg, J. J.: Chemoautotrophy in the ocean, *Geophys. Res. Lett.*, 38, 94–97, <https://doi.org/10.1029/2011GL049725>, 2011.
- Mincer, T. J., Church, M. J., Taylor, L. T., Preston, C., Karl, D. M., and DeLong, E. F.: Quantitative distribution of presumptive archaeal and bacterial nitrifiers in Monterey Bay and the North Pacific Subtropical Gyre, *Environ. Microbiol.*, 9, 1162–1175, <https://doi.org/10.1111/j.1462-2920.2007.01239.x>, 2007.
- Olsen, R.: Differential photoinhibition of marine nitrifying bacteria: a possible mechanism for the formation of the primary nitrite maximum, *J. Marine Syst.*, 31, 227–238, 1989.
- Pachiadaki, M. G., Sintès, E., Bergauer, K., Brown, J. M., Record, N. R., Swan, B. K., Mathyer, M. E., Hallam, S. J., Lopez-Garcia, P., Takaki, Y., Nunoura, T., Woyke, T., Herndl, G. J., and Stepanauskas, R.: Major role of nitrite-oxidizing bacteria in dark ocean carbon fixation, *Science*, 358, 1046–1051, <https://doi.org/10.1126/science.aan8260>, 2017.
- Rahav, E., Herut, B., Mulholland, M. R., Belkin, N., Elifantz, H., and Berman-Frank, I.: Heterotrophic and autotrophic contribution to dinitrogen fixation in the Gulf of Aqaba, *Mar. Ecol. Prog. Ser.*, 522, 67–77, <https://doi.org/10.3354/meps11143>, 2015.
- Reich, T., Belkin, N., Sisma-Ventura, G., Berman-Frank, I., and Rahav, E.: Significant dark inorganic carbon fixation in the euphotic zone of an oligotrophic sea, *Limnol. Oceanogr.*, 9999, 1–14, <https://doi.org/10.1002/Ino.12560>, 2024.
- Reich, T., Belkin, N., Sisma-Ventura, G., Hauzer, H., Rubin-Blum, M., Berman-Frank, I., and Rahav, E.: Contribution of dark inorganic carbon fixation to bacterial carbon demand in the oligotrophic Southeastern Mediterranean Sea, *Ocean Sci.*, 21, 3055–3067, <https://doi.org/10.5194/os-21-3055-2025>, 2025.
- Reich, T., Belkin, N., Sisma-ventura, G., Hauzer, H., Berman-frank, I., and Rahav, E.: Does oligotrophy favor chemoautotrophy over photoautotrophy, *Prog. Oceanogr.*, 241, 103633, <https://doi.org/10.1016/j.pocean.2025.103633>, 2026.
- Santoro, A. E., Casciotti, K. L., and Francis, C. A.: Activity, abundance and diversity of nitrifying archaea and bacteria in the central California current, *Environ. Microbiol.*, 12, 1989–2006, <https://doi.org/10.1111/j.1462-2920.2010.02205.x>, 2010.
- Scofield, A. E., Watkins, J. M., Osantowski, E., and Rudstam, L. G.: Deep chlorophyll maxima across a trophic state gradient: A case study in the Laurentian Great Lakes., *Limnol. Oceanogr.*, 65, 2460–2484, <https://doi.org/10.1002/Ino.11464>, 2020.
- Shafiee, R. T., Snow, J. T., Zhang, Q., and Rickaby, R. E. M.: Iron requirements and uptake strategies of the globally abundant marine ammonia-oxidising archaeon, *Nitrosopumilus maritimus* SCM1, *ISME J.*, 13, 2295–2305, <https://doi.org/10.1038/s41396-019-0434-8>, 2019.
- Shafiee, R. T., Diver, P. J., Snow, J. T., Zhang, Q., and Rickaby, R. E. M.: Marine ammonia-oxidising archaea and bacteria occupy distinct iron and copper niches, *ISME Commun.*, 1, 1, <https://doi.org/10.1038/s43705-021-00001-7>, 2021.
- Shiozaki, T., Ijichi, M., Fujiwara, A., Makabe, A., Nishino, S., Yoshikawa, C., and Harada, N.: Factors regulating nitrification in the Arctic Ocean: potential impact of sea ice reduction and ocean acidification, *Global Biogeochem. Cy.*, 33, 1085–1099, <https://doi.org/10.1029/2018GB006068>, 2019.
- Sigman, D. M., Casciotti, K. L., Andreani, M., Barford, C., Galanter, M., and Böhlke, J. K.: A bacterial method for the nitrogen isotopic analysis of nitrate in seawater and freshwater, *Anal. Chem.*, 73, 4145–4153, <https://doi.org/10.1021/ac010088e>, 2001.
- Smith, J. M., Chavez, F. P., and Francis, C. A.: Ammonium Uptake by Phytoplankton Regulates Nitrification in the Sunlit Ocean, *PLoS ONE*, 9, e108173, <https://doi.org/10.1371/journal.pone.0108173>, 2014.
- Smith, J. M., Damashek, J., Chavez, F. P., and Francis, C. A.: Factors influencing nitrification rates and the abundance and transcriptional activity of ammonia-oxidizing microorganisms in the dark northeast Pacific Ocean, *Limnol. Oceanogr.*, 61, 596–609, <https://doi.org/10.1002/Ino.10235>, 2016.

- Stambler, N.: Light and picophytoplankton in the Gulf of Eilat (Aqaba), *J. Geophys. Res.*, 111, C11009, <https://doi.org/10.1029/2005JC003373>, 2006.
- Stambler, N.: Underwater light field of the Mediterranean Sea, in: *Life in the Mediterranean Sea: A Look at Habitat Changes*, edited by: Stambler, N., Nova Science Publishers, 1–739, ISBN 978-1-61209-644-5, 2012.
- Steemann-Nielsen, E.: The use of radioactive carbon ( $^{14}\text{C}$ ) for measuring organic production in the sea, *J. des Cons. Int. Pour Explor. la Mer*, 18, 117–140, 1952.
- Stukel, M. R.: Investigating equations for measuring dissolved inorganic nutrient uptake in oligotrophic conditions, *Limnol. Oceanogr.-Meth.*, 18, 656–672, 2020.
- Suggett, D. J., Stambler, N., Prášil, O., Kolber, Z., Quigg, A., Vázquez-Domínguez, E., Zohary, T., Berman, T., Iluz, D., Levitan, O., Lawson, T., Meeder, E., Lazar, B., Bar-Zeev, E., Medova, H., and Berman-Frank, I.: Nitrogen and phosphorus limitation of oceanic microbial growth during spring in the Gulf of Aqaba, *Aquat. Microb. Ecol.*, 56, 227–239, 2009.
- Tang, W., Ward, B. B., Beman, M., Bristow, L., Clark, D., Fawcett, S., Frey, C., Fripiat, F., Herndl, G. J., Mdutyana, M., Paulot, F., Peng, X., Santoro, A. E., Shiozaki, T., Sintès, E., Stock, C., Sun, X., Wan, X. S., Xu, M. N., and Zhang, Y.: Database of nitrification and nitrifiers in the global ocean, *Earth Syst. Sci. Data*, 15, 5039–5077, <https://doi.org/10.5194/essd-15-5039-2023>, 2023.
- Torfstein, A., Teutsch, N., Tirosch, O., Shaked, Y., Rivlin, T., Zippori, A., Stein, M., Lazar, B., and Erel, Y.: Chemical characterization of atmospheric dust from a weekly time series in the north Red Sea between 2006 and 2010, *Geochim. Cosmochim. Ac.*, 211, 373–393, <https://doi.org/10.1016/j.gca.2017.06.007>, 2017.
- Travis, N. M., Kelly, C. L., and Casciotti, K. L.: Testing the influence of light on nitrite cycling in the eastern tropical North Pacific, *Biogeosciences*, 21, 1985–2004, <https://doi.org/10.5194/bg-21-1985-2024>, 2024.
- Wan, X. S., Sheng, H.-X., Dai, M., Church, M. J., Zou, W., Li, X., Hutchins, D. A., Ward, B. B., and Kao, S.-J.: Phytoplankton-nitrifier interactions control the geographic distribution of nitrite in the upper ocean, *Global Biogeochem. Cy.*, 35, e2021GB007072, <https://doi.org/10.1029/2021GB007072>, 2021.
- Wan, X. S., Sheng, H.-X., Shen, H., Zou, W., Tang, J.-M., Qin, W., Dai, M., Kao, S.-J., and Ward, B. B.: Significance of Urea in Sustaining Nitrite Production by Ammonia Oxidizers in the Oligotrophic Ocean, *Global Biogeochem. Cy.*, 38, e2023GB007996, <https://doi.org/10.1029/2023GB007996>, 2024.
- Wankel, S. D., Kendall, C., Pennington, J. T., Chavez, F. P., and Paytan, A.: Nitrification in the euphotic zone as evidenced by nitrate dual isotopic composition: Observations from Monterey Bay, California, *Global Biogeochem. Cy.*, 21, 1–13, <https://doi.org/10.1029/2006GB002723>, 2007.
- Ward, B. B.: Light and substrate concentration relationships with marine ammonium assimilation and oxidation rates, *Mar. Chem.*, 16, 301–316, [https://doi.org/10.1016/0304-4203\(85\)90052-0](https://doi.org/10.1016/0304-4203(85)90052-0), 1985.
- Ward, B. B.: Nitrogen transformations in the Southern California Bight, *Deep-Sea Res. Pt. I*, 34, 785–805, [https://doi.org/10.1016/0198-0149\(87\)90037-9](https://doi.org/10.1016/0198-0149(87)90037-9), 1987.
- Ward, B. B.: Nitrification in Marine Systems, in: *Nitrogen in the Marine Environment Environment*, edited by: Capon, D. G., Bronk, D. A., Mulholland, M. R., and Carpenter, E. J., Elsevier, 199–262, <https://doi.org/10.1016/B978-0-12-372522-6.00005-0>, 2008.
- Welschmeyer, N. A.: Fluorometric analysis of chlorophyll-*a* in the presence of chlorophyll-*b* and pheopigments, *Limnol. Oceanogr.*, 39, 1985–1992, 1994.
- Wuchter, C., Abbas, B., Coolen, M. J. L., Herfort, L., van Bleijswijk, J., Timmers, P., Strous, M., Teira, E., Herndl, G. J., Middelburg, J. J., Schouten, S., and Sinninghe Damsté, J. S.: Archaeal nitrification in the ocean, *P. Natl. Acad. Sci. USA*, 103, 12317–12322, <https://doi.org/10.1073/pnas.0600756103>, 2006.
- Xu, M. N., Li, X., Shi, D., Zhang, Y., Dai, M., Huang, T., Glibert, P. M., and Kao, S.-J.: Coupled effect of substrate and light on assimilation and oxidation of regenerated nitrogen in the euphotic ocean, *Limnol. Oceanogr.*, 64, 1270–1283, <https://doi.org/10.1002/lno.11114>, 2019.
- Yin, Q., He, K., Collins, G., De Vrieze, J., and Wu, G.: Microbial strategies driving low concentration substrate degradation for sustainable remediation solutions, *npj Clean Water*, 7, 52, <https://doi.org/10.1038/s41545-024-00348-z>, 2024.
- Yool, A., Martin, A. P., Fernández, C., and Clark, D. R.: The significance of nitrification for oceanic new production, *Nature*, 447, 999–1002, <https://doi.org/10.1038/nature05885>, 2007.
- Zheng, Z.-Z., Wan, X., Xu, M. N., Hsiao, S. S.-Y., Zhang, Y., Zheng, L.-W., Wu, Y., Zou, W., and Kao, S.-J.: Effects of temperature and particles on nitrification in a eutrophic coastal bay in southern China, *J. Geophys. Res.-Biogeo.*, 122, 2325–2337, <https://doi.org/10.1002/2017JG003871>, 2017.
- Zheng, Z.-Z., Zheng, L.-W., Xu, M. N., Tan, E., Hutchins, D. A., Deng, W., Zhang, Y., Shi, D., Dai, M., and Kao, S.-J.: Substrate regulation leads to differential responses of microbial ammonia-oxidizing communities to ocean warming, *Nat. Commun.*, 11, 3511, <https://doi.org/10.1038/s41467-020-17366-3>, 2020.
- Zhou, Y., Yan, A., Yang, J., He, W., Guo, S., Li, Y., Wu, J., Dai, Y., Pan, X., Cui, D., Pereira, O., Teng, W., Bi, R., Chen, S., Fan, L., Wang, P., Liao, Y., Qin, W., Sui, S.-F., Zhu, Y., Zhang, C., and Liu, Z.: Ultrastructural insights into cellular organization, energy storage and ribosomal dynamics of an ammonia-oxidizing archaeon from oligotrophic oceans, *Front. Microbiol.*, 15, 1367658, <https://doi.org/10.3389/fmicb.2024.1367658>, 2024.
- Zhu, W., Wang, C., Hill, J., He, Y., Tao, B., Mao, Z., and Wu, W.: A missing link in the estuarine nitrogen cycle? Coupled nitrification-denitrification mediated by suspended particulate matter, *Sci. Rep.*, 8, 2282, <https://doi.org/10.1038/s41598-018-20688-4>, 2018.